# Simultaneous Facility Location and Path Optimization in Static and Dynamic Networks

Amber Srivastava and Srinivasa M. Salapaka, *Member, IEEE*

***Abstract*—We present a framework for solving simultaneously the problems of facility location and path optimization in static and dynamic spatial networks. In the static setting, the objective is to determine facility locations and transportation paths from each node to the destination via the network of facilities such that the total cost of commodity transportation is minimized. This is an NP-hard problem. We propose a novel stage-wise viewpoint of the paths which is instrumental in designing the decision variable space in our framework. We use the maximum entropy principle to solve the resulting optimization problem. In the dynamic setting, nodes and destinations are dynamic. We design an appropriate control Lyapunov function to determine the time evolution of facilities and paths such that the transportation cost at each time instant is minimized. Our framework enables quantifying attributes of the facilities and transportation links in terms of the decision variables. Consequently, it becomes possible to incorporate application specific constraints on individual facilities, links, and network topology. We demonstrate the efficacy of our proposed framework through extensive simulations.**

***Index Terms*—Dynamic programming, facility location, maximum entropy principle (MEP), shortest path, spatial network.**

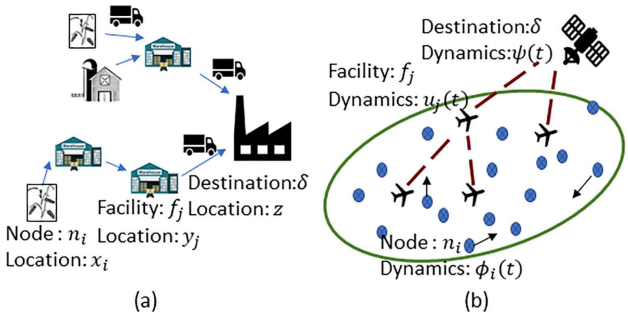


Fig. 1. (a) Agricultural supply chain which comprises of several farm nodes $n_i$ which transport commodities to the processing unit $\delta$ through a network of warehouses $f_j$. Objective is to determine warehouse locations $\{y_j\}$ and design relevant transportation paths. (b) Battlefield Surveillance - comprises of several nodes $n_i$ (with dynamics $\phi_i(t)$) which communicates with the satellite $\delta$ (with dynamics $\psi(t)$) through a network of facilities $f_j$. Objective is to find the dynamics of the facility locations $\{u_j(t)\}$ and time-varying communication paths.

## I. Introduction

MANY complex systems are modeled as spatial graphs where nodes are embedded into a metric space [1]–[5]. Areas, such as supply chain networks [6]; vehicle routing [7]; industrial process monitoring and power grids [8]; battlefield surveillance [9]; disaster management [10], [11]; small cell network design in 5G networks [12]; wireless networks [13], [14]; and last mile delivery [15], come under the purview of spatial networks. Often in these areas a large number of spatially scattered nodes need to transport a commodity (such as information, raw, or processed goods) to a given destination (or central processing center). Cost and implementation considerations in these large networks result in nodes that can transport only to nearby locations. This drawback is addressed by overlaying a much smaller network of facilities (special nodes) where each facility has the resources to transport commodities to other facilities even if they are far. These facilities also have resources to collect commodities from the nearby nodes. Thus, a typical transportation path in such a network would start at a node, go through the network of facilities, and culminate at a destination node [see Fig. 1(a)]. Therefore, designing of such a network requires placement of facilities that *cover* all the nodes and determining the shortest transportation path from each node to the respective destination center.

The problem in the context of overlaying the network of facilities over the network of nodes can be described in terms of the following two objectives: 1) find locations of facilities that cover a large set of underlying nodes and 2) design the shortest transportation path from each node, via the network of facilities, to the destination center such that the total cost of transportation is minimized. For instance, Fig. 1(a) illustrates an agricultural supply chain where the farm nodes $n_i$, located at $x_i$, need to transport produce to a food processing center $\delta$ located at $z$ through the network of warehouses $\{f_j\}$. To minimize the cost incurred in the supply chain, the warehouse locations $\{y_j\}$ and the transportation path from each farm node $n_i$ to the processing center $\delta$ needs to be determined. Since all of the nodes, destination center, and the facilities are static in this problem, we refer to it as simultaneous facility location and path optimization in static spatial networks, abbreviated as $s$-FLPO.

Manuscript received November 14, 2019; revised February 12, 2020; accepted May 1, 2020. Date of publication May 19, 2020; date of current version December 16, 2020. This work was supported in part by NSF under Grant CNS 1544635 and in part by ECCS (NRI) under Grant 18-30639. This article was presented in part at the Indian Control Conference, Delhi, India, January 2019. Recommended by Associate Editor M. Prandini. *(Corresponding author: Amber Srivastava.)*

The authors are with the Department of Mechanical Engineering, University of Illinois at Urbana-Champaign, Urbana, IL 61801 USA (e-mail: asrvstv6@illinois.edu; salapaka@illinois.edu).

Digital Object Identifier 10.1109/TCNS.2020.2995831

In many application areas, such as battlefield reconnaissance and disaster management, the nodes and the destination center have associated dynamics. For instance, Fig. 1(b) illustrates a scenario of battlefield surveillance where each node $n_i$, with dynamics $\phi_i(t)$, investigates the domain $\Omega$ and communicates the relevant information in real time to the satellite $\delta$ with dynamics $\psi(t)$. The communication is facilitated through a network of unmanned aerial vehicles (UAVs) $\{f_j\}$ and the objective is to minimize the total cost of communication at each time instant. This task requires determining the appropriate dynamics $u_j(t)$ of each UAV $f_j$ as well as the time-varying optimal communication paths. We refer to this problem as the simultaneous facility location and path optimization in dynamic spatial networks, abbreviated as *d*-FLPO.

The goal of the facility location problem in *s*-FLPO is to allocate a set of facilities $\{y_j\}$ to data points $\{x_i\}$ such that the cumulative distance between data points and their nearest facility is minimized. This is an NP-hard problem [16]. Another aspect of *s*-FLPO is the shortest path design problem on a network graph $G(V, E)$ which aims to find a minimum cost path between any two vertices $v_1, v_2 \in V$. This problem is solvable in polynomial order of vertices and edges [17]. The additional objective of determining the shortest path adds to the inherent complexity of the facility location problem thereby resulting into a much more complex *s*-FLPO problem where the cost functions are riddled with multiple poor local minima. A straightforward method to solve the *s*-FLPO problem would be to sequentially solve facility location, and shortest path problems as done in [7] in the context of multidepot vehicle routing. However, owing to the fact that the two subproblems are coupled, such a sequential methodology results in a solution with a much larger cost function value as demonstrated later in our simulations.

There is extensive literature that addresses the facility location problem [18]–[24] and the shortest path problem [25]–[27] individually. But there is scant literature that solves the two problems simultaneously. Our previous works in [28] and [29] are, to the best of our knowledge, the only efforts along this direction in the context of spatial networks. However, the framework proposed in [28] does not scale with the number of facilities $M$ and the corresponding algorithm becomes computationally intractable even for small values of $M(\geq 15)$. This is because the framework in [28] views every permutation and combination of the $M$ facilities as a feasible transportation path and requires each such path to be represented by a separate decision variable; resulting into a combinatorially large $\mathcal{O}(\sum_{k=1}^{M} \binom{M}{k} k!)$ decision variable space. In addition to that, the decision variables in [28] fail to provide any *quantitative* insight at the level of the individual facilities $\{f_j\}$ and the transportation links $\{(f_i, f_j)\}$ such as the usage of a particular facility or a transportation link; because of this, the framework in [28] is not flexible to incorporate application-specific capacity-based constraints on the facilities and network topology.

On the other hand, the framework proposed in [29], though scalable with decision variable space growing polynomially $\mathcal{O}(M^2)$, is applicable to only a restricted class of FLPO problems where all the transportation paths assume a specific structure. As a consequence of this structure, the framework in [29] prohibits all such paths where two distinct facilities $f_{j_1}$ and $f_{j_2}$ establish a transportation link concurrently with the same facility $f_{j_3}$. The set of all feasible paths in [29] consists of only a few *ordered* sequences of facilities where no facility can lie in more than one sequence. Though enforcing the above path structure in [29] over [28] reduces the decision variable space from combinatorially large $\mathcal{O}(\sum_{k=1}^{M} \binom{M}{k} k!)$ to polynomial size $\mathcal{O}(M^2)$, it results into suboptimal solutions when used for the general class of FLPO problems that do not necessitate the path structure assumed in [29]. We demonstrate this via simulations in a later section.

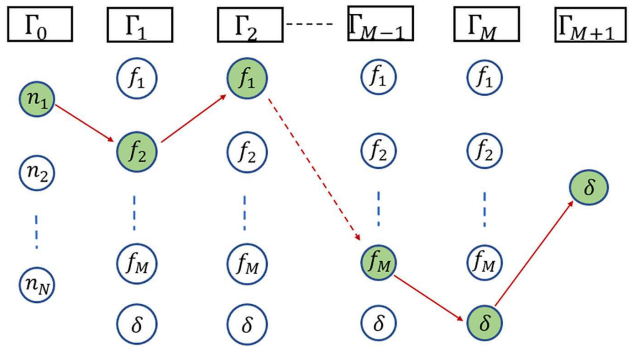


Fig. 2. Transportation path $\gamma$ from the node $n_1 \in \Gamma_0$ to the destination $\delta \in \Gamma_{M+1}$ via the stages $\{\Gamma_k\}_{k=1}^{M}$.

In this work, we develop a scalable framework for the general class of *s*-FLPO problem to overcome the limitations of [28] and [29]. We achieve this by developing a novel stage-wise viewpoint of the transportation paths (see Fig. 2) and exploiting the constraint resulting from the nature of *optimal* transportation paths. More specifically, the stage-wise viewpoint of the paths allows us to impose the structure on the design of decision variables that results from the law of optimality, that is, when any two optimal transportation paths in the network intersect at a particular stage then the subsequent route from the facility at that stage to the destination will be the same for both paths. The stage-wise viewpoint is the main mechanism that allows for substantial reduction in the size of decision variable space from $\mathcal{O}(\sum_{k=1}^{M} \binom{M}{k} k!)$ in [28] to the order $\mathcal{O}(M^3)$ in the current work without enforcing any path structure as in [29].

One of the salient features resulting from our stage-wise illustration of the transportation paths is that it provides quantitative insights into several parameters of the *s*-FLPO problem in terms of the underlying decision variables. For instance, quantities such as the number of transportation paths using a particular facility $f_j$ in a particular stage, fraction of nodes connected directly to a given facility, and number of paths that include a particular transportation link $(f_i, f_j)$ at a particular stage can be efficiently expressed in terms of the stage-wise decision variables. Note that once quantifiable in terms of the decision variables, it is easier to specify application-specific constraints on all such parameters. In addition, we demonstrate the flexibility of our proposed framework to incorporate various such capacity constraints on facilities, transportation paths, and the network topology. We illustrate this using networks where: 1) the maximum length of

the transportation paths are restricted; 2) the network is partially connected; and/or 3) the facilities and the transportation *links* have maximum associated capacities. It must be noted that incorporating these constraints causes no considerable changes in the algorithm, making their implementation straightforward.

In the context of the *d*-FLPO problem, we show that the relaxed cost function that appears in the solution framework of the *s*-FLPO problem serves as a good candidate for a control-Lyapunov function. We design a control law for the dynamics $\{u_j(t)\}$ of the facilities which ensures that the time-derivative of this Lyapunov function remains nonpositive at all times. The time-varying transportation paths are then determined using the facility locations $\{y_j(t)\}$ at each time instant. The important aspects of our control design that we show are: 1) the *asymptotic tracking* of the local minimum to *d*-FLPO problem (Theorem 3) and 2) *nonconservative* property (Theorem 4), i.e., if there exists a Lipschitz control law that asymptotically tracks the local optimal of the *d*-FLPO problem then the proposed control law is also Lipschitz and bounded.

We present extensive simulations for the *s*-FLPO problem in unconstrained and constrained scenarios to demonstrate the efficacy of our algorithm in terms of scalability, time-complexity, and the quality of solutions. Also, a wide range of constraints on the facilities, transportation path, and network topology are demonstrated in our simulations. We demonstrate the efficacy of our framework on a large-scale system with approximately N = 17 000 nodes and allocate $M = 50$ facilities with the cost function values that are approximately 25% better than the solution obtained using [29]; note that the framework in [28] results in $(\approx)10^{64}$ decision variables for this scenario and hence the corresponding algorithm is severely intractable.

We compare our simulations of the *d*-FLPO problem with the *frame-by-frame* approach where we solve the *s*-FLPO problem at each time instant to estimate the dynamics of the facilities and transportation paths. We show the considerable benefits of our proposed methodology obtained with respect to algorithmic run times and practicality of the dynamics of the facilities in comparison to the frame-by-frame approach. The computational times are significantly reduced; as much as by 700 times have been demonstrated. Also, the simulations show that the frame-by-frame approach requires some facilities to undergo a considerable spatial change in a very small interval of time thereby resulting into a nonviable dynamics which do not occur when using our methodology.

## II. *s*-FLPO Problem

The *s*-FLPO problem is characterized by overlaying a network of $M$ facilities on a network of large number $N \gg M$ of nodes and designing a path (single or multihop) from each node to the destination via the network of facilities. Let the node $n_i$ be located at $x_i \in \mathbb{R}^d$, $1 \leq i \leq N$, and the destination $\delta$ be located at $z \in \mathbb{R}^d$. Let $\Gamma_0 = \{n_1, \ldots, n_N\}$ denote the set of all nodes. The twofold objective of the optimization problem is to determine the location $y_j \in \mathbb{R}^d$ of the facilities $f_j$, $1 \leq j \leq M$ and design transportation paths from each node $n_i$ to the destination $\delta$ via the network of facilities such that the total cost of transportation (as quantified later in this section) is minimized. A transportation path

$$n_i \to f_{r_1} \to f_{r_2} \to \cdots \to f_{r_q} \to \delta \tag{1}$$

where $r_j \in \{1, \ldots, M\}$, from the node $n_i \in \Gamma_0$ to the destination $\delta$ is an ordered sequence of $q$ $(\leq M)$ distinct facilities. For such a path, we say that the path length (or number of hops) is $q$. In our framework, we model a transportation path $\gamma$ from a node $n_i \in \Gamma_0$ to the destination $\delta$ as a sequence

$$\gamma = (\gamma_1, \ldots, \gamma_M) \tag{2}$$

where $\gamma_k \in \Gamma_k \ \forall \ 1 \leq k \leq M$. Here the stage $\Gamma_k$ is the collection of all the facilities and the destination center, that is, $\Gamma_k = \{f_1, \ldots, f_M, \delta\} \ \forall \ 1 \leq k \leq M$ (see Fig. 2). For the transportation path in (1) $\gamma_k = f_{r_k} \ \forall \ k \in \{1, \ldots, q\}$ and $\gamma_k = \delta \ \forall \ k \in \{q+1, \ldots, M\}$, i.e., in our representation of a transportation path we pad (1) with $M - q$ many $\delta$'s at the end. We define $\Gamma_{M+1} := \{\delta\}$ as a singleton set comprising of the destination center and $\mathcal{G} := \{(\gamma_1, \ldots, \gamma_M) : \gamma_k \in \Gamma_k \forall 1 \leq k \leq M\}$ as the set of all possible transportation paths. Please refer to Fig. 2 for a pictorial illustration of a transportation path from $n_1 \in \Gamma_0$ to destination $\delta \in \Gamma_{M+1}$ via the stages $\{\Gamma_k\}_{k=1}^{M}$. The objective of the *s*-FLPO problem is to

$$\min_{\substack{\{y_j\} \\ 1 \leq j \leq M}} D_0 := \sum_{\gamma_0 \in \Gamma_0} \left[ \rho_{\gamma_0} \sum_{\gamma \in \mathcal{G}} \nu(\gamma|\gamma_0) d(\gamma_0, \gamma) \right] \tag{3}$$

where $\rho_{\gamma_0}$ is a given relative weight of the node $\gamma_0 \in \Gamma_0$

$$\nu(\gamma|\gamma_0) = \begin{cases} 1, & \text{if } \gamma = \arg\min_{\gamma' \in \mathcal{G}} d(\gamma_0, \gamma') \\ 0, & \text{otherwise} \end{cases} \tag{4}$$

and $d(\gamma_0, \gamma) = \sum_{k=0}^{M} d_k(\gamma_k, \gamma_{k+1})$ is the cost incurred along the path $\gamma = (\gamma_1, \ldots, \gamma_M)$ from the node $\gamma_0$ to the destination $\delta$. Here $d_k(\cdot, \cdot)$ represents the cost of transportation from the stage $\Gamma_k$ to $\Gamma_{k+1}$. For notational simplicity we denote $d_k(\gamma_k, \gamma_{k+1})$ as $d_k$ wherever clear from the context. The framework presented in this article is applicable to any general cost function $d_k(\gamma_k, \gamma_{k+1})$; however, for the purpose of illustration we assume it to be the squared Euclidean distance, i.e., $d_k(\gamma_k, \gamma_{k+1}) = \|y_{r_k} - y_{r_{k+1}}\|^2$, where $\gamma_k = f_{r_k}$, $\gamma_{k+1} = f_{r_{k+1}}$.

## III. Solution to *s*-FLPO Problem

A straightforward approach to solving the twofold objective optimization problem (3) is to solve for the two objectives sequentially, i.e., first allocate facilities to the nodes using any of the facility location algorithms mentioned in Section I and then find the shortest transportation path from each node to the destination by solving the shortest path problem on the resulting network graph [30]. However, this approach disregards the fact that the two objectives are coupled and therefore result in a suboptimal solution. Also, the algorithms mentioned in Section I, which solve the facility location problem, are substantially dependent on the initialization step. For instance, in Lloyd's algorithm (or $k$-means algorithm) [23], [31], the initial step consists of randomly choosing facility locations to form the initial facility locations. Since the iterative scheme is such that

only the "proximal" input points determine the facility location and not the "distant" input points, the $k$-means algorithm has a tendency to get trapped in the local minima.

The algorithm that we propose in this work is motivated from the deterministic annealing (DA) algorithm for the facility location problem [22]. In particular, the proposed algorithm overcomes the local influence of the nodes on the solution to $s$-FLPO problem by associating each node $\gamma_0$ with all transportation paths through a weighting parameter $p(\gamma|\gamma_0)$. Without loss of generality, we assume that $\sum_{\gamma\in\mathcal{G}} p(\gamma|\gamma_0) = 1 \; \forall \; \gamma_0 \in \Gamma_0$ and the proposed algorithm seeks to minimize the relaxed version of the cost function in (3) given by

$$D = \sum_{\gamma_0\in\mathcal{S}} \rho_{\gamma_0} \sum_{\gamma\in\mathcal{G}} p(\gamma|\gamma_0) d(\gamma_0,\gamma). \tag{5}$$

It must be noted that the choice of association weights $p(\gamma|\gamma_0)$ determines the tradeoff between the local influence (or the initialization of the algorithm) and deviation from the original cost function (3), i.e., if the association weights are uniformly distributed $p(\gamma|\gamma_0) = 1/|\mathcal{G}|$, then the two cost functions differ largely from each other; however, the minimization of the objective function (5) is independent of the initialization of the algorithm as all possible paths from the nodes $\gamma_0$ are given equal weights. For the choice of association weights $p(\gamma|\gamma_0) = \nu(\gamma|\gamma_0)$, the relaxed cost function (5) reduces back to the original cost function (3).

It follows from the *law of optimality* that along an optimal transportation path, the upcoming facility on the path is decided solely by the current facility and is independent of the prior facilities on that path. We impose this structure on our choice of the association weights $p(\gamma|\gamma_0)$, which translates to a Markov property. Thus, the association weight $p(\gamma|\gamma_0)$, which relates an entire transportation path $\gamma = (\gamma_1,\ldots,\gamma_M)$ to the node $\gamma_0$, can be broken down into association weights $\{p_k(\gamma_{k+1}|\gamma_k)\}_{k=1}^{M}$, where $p_k(\gamma_{k+1}|\gamma_k)$ relates the stage $\Gamma_k$ to $\Gamma_{k+1}$. More specifically

$$p(\gamma|\gamma_0) = \prod_{k=0}^{M} p_k(\gamma_{k+1}|\gamma_k). \tag{6}$$

For notational simplicity, we denote $p_k(\gamma_{k+1}|\gamma_k)$ as $p_k$ whenever it is clear from the context. The association weights $p_k(\gamma_{k+1}|\gamma_k) \; \forall \; 0 \le k \le M-1$ along with the spatial coordinates $\{y_j\}$, $1 \le j \le M$ of the facilities comprise the decision variable space of our optimization problem. The relaxed cost function in (5) is now rewritten as

$$D = \sum_{\gamma_0\in\Gamma_0} \rho_{\gamma_0} \sum_{\gamma\in\mathcal{G}} \prod_{k=0}^{M} p_k d(\gamma_0,\gamma). \tag{7}$$

Observe that the decision variable $p(\gamma|\gamma_0)$ in (5) is replaced by the decision variable $p_k(\gamma_{k+1}|\gamma_k)$ in (7), thereby making our optimization problem across all possible paths $\gamma$ to an optimization problem across consecutive stages $\Gamma_k$ and $\Gamma_{k+1}$, $1 \le k \le M$. This results in the reduction of decision variable space from $O(\sum_{k=1}^{M} \binom{M}{k} k!)$ to $O(M^3)$.

We use the maximum entropy principle (MEP) [32], [33] to design the association weights $p_k(\gamma_{k+1}|\gamma_k)$ such that the cost function (7) attains a specified value. More specifically, MEP determines the association weights by solving the following associated optimization problem:

$$\max_{\{p_k\}} H := -\sum_{\gamma_0\in\mathcal{S}} \rho_{\gamma_0} \sum_{\gamma\in\mathcal{G}} \left(\prod_{k=0}^{M-1} p_k\right) \log\left(\prod_{k=0}^{M-1} p_k\right) \tag{8}$$

$$\text{s.t. } D = c_0 \tag{9}$$

where $c_0$ is a given value of the cost function. This problem is solved repeatedly at decreasing values of $c_0$, which is described later in Section III. As the entropy term (8) quantifies for the level of randomness, maximizing it at a fixed value $c_0$ of the cost function (7) results into association weights $p_k(\gamma_{k+1}|\gamma_k)$ that ensures maximum uncertainty or uncommitted nature of the algorithm toward any particular solution. The Lagrangian corresponding to the optimization problem in (8) and (9) is given by

$$\bar{F} = (D - c_0) - \frac{1}{\beta} H \tag{10}$$

where $1/\beta$ is the Lagrange multiplier. The Lagrangian $\bar{F}$ is convex in $p_k \; \forall \; k$ and we determine the association weights by setting $\frac{\partial \bar{F}}{\partial p_k} = 0$ which yields

$$p_k = \left(e^{-\beta d_k}\right) \frac{\sum_{\substack{(\sigma_{k+2},\ldots,\sigma_M):\\ \sigma_{k+1}=\gamma_{k+1}}} e^{-\beta \sum_{t=k+1}^{M} d_t(\sigma_t,\sigma_{t+1})}}{\sum_{\substack{(\sigma_{k+1},\ldots,\sigma_M):\\ \sigma_k=\gamma_k}} e^{-\beta \sum_{t=k}^{M} d_t(\sigma_t,\sigma_{t+1})}}. \tag{11}$$

In the expression of the unconstrained Lagrangian (10), we refer to the lagrange parameter $\frac{1}{\beta}$ as the *temperature* and $\bar{F}$ as the *Free energy* because of their close analogies to statistical physics [where free energy is enthalpy (D) minus the temperature times entropy (TH)]. Substituting (11) into the expression of *free energy* $\bar{F}$ in (10), we obtain

$$F = -\frac{1}{\beta} \sum_{\gamma_0\in\Gamma_0} \rho_{\gamma_0} \log \sum_{\gamma\in\mathcal{G}} e^{-\beta \sum_{t=0}^{M} d_t(\gamma_t,\gamma_{t+1})}. \tag{12}$$

Note that for brevity we ignore the constant term $c_0$ in the above expression of $F$. As illustrated later the Lagrange parameter $\beta$ implicitly decides the value of $c_0$. Additionally, the above $F$ can be viewed as a relaxation of the cost function $D$ in (7). In fact, as $\beta \to \infty$ we observe that $F \to D$. We now minimize (locally) $F$ in (12) with respect to $y = [y_1^T,\ldots,y_M^T]^T$ to obtain the spatial coordinates of the facilities, i.e., we put $\frac{\partial F}{\partial y} = 0$ to obtain

$$y = (2\hat{A} - \hat{B})^{-1}(\hat{\bar{X}} + \hat{C}) \tag{13}$$

where $\hat{A} = I_d \otimes A$, $\hat{B} = I_d \otimes B$, $\hat{\bar{X}} = I_d \otimes \bar{X}$, $\hat{C} = I_d \otimes C$, and $I_d$ is an identity matrix of $d \times d$ dimension. The matrices $A, B \in \mathbb{R}^{M\times M}$, $\bar{X}, C \in \mathbb{R}^{M\times d}$ depend on the association weights $p_k(\gamma_{k+1}\gamma_k)$, the spatial coordinates of the nodes $\{x_i\}$ and the destination location $z$. Please refer to the Appendix A for the definitions of the above matrices and the proof that the matrix $(2\hat{A} - \hat{B})$ is positive definite (i.e., invertible).

**Algorithm 1:** main($X$, $z$, $\beta_{\min}$, $\beta_{\max}$).

1: Initialize $\beta$ to the small value $\beta_{\min}$.
2: Calculate the association weights $\{p_k(\gamma_{k+1}|\gamma_k)\}$ in (11).
3: Calculate the facility locations $y$ in (13).
4: Iterate between step 2 and 3 until convergence.
5: Increase $\beta$ by a factor $\kappa > 1$; i.e., $\beta \leftarrow \kappa\beta$.
6: Stop if $\beta \geq \beta_{\max}$. Else go to step 2.

The constraint value $c_0$ in (9) decides the temperature variable $T = 1/\beta$. It follows from the sensitivity analysis [34] that the lower value of $c_0$ corresponds to the higher value of $\beta$. It is clear from (10) that for small values of $\beta$ (i.e., high values of $c_0$), we are mainly minimizing the convex function $-H$, which results in uniformly distributed association weights. As $\beta$ increases ($c_0$ decreases), more and more weightage in (10) is given to the cost function $D$, i.e., $F$ closely approximates the nonconvex cost function $D$. In the limit $\beta \to \infty$, we have that $F = D$ and we obtain hard association weights $p_k(\gamma_{k+1}|\gamma_k) \in \{0, 1\}$. The idea is essentially to find the global minimum of the convex function $-H$ and then track the minimum of $F$ at successively increasing values of $\beta$, until $F \to D$. This is done in our algorithm via iterating between (11) and (13) at a successively increasing value of $\beta$, and using the solution from each $\beta$ iteration as an initialization for the next $\beta$ iteration. The resulting annealing algorithm is as follows.

***Theorem 1:*** The iterations in step 4 of the Algorithm 1 are equivalent to iterations of a descent method to solve the implicit equation (13). Consequently Algorithm 1 converges.

Please refer to the Appendix B for the proof.

## IV. Phase Transition Phenomenon

The above algorithm upon implementation exhibits *phase transitions* very similar to that seen when DA [22] is applied to pure facility location problems. In the initial iterations of the algorithm when $\beta$ is very small, the cost function is dominated by $-H$; minimizing this gives uniform distributions for the association weights $p_k(\gamma_{k+1}|\gamma_k)$. Also with this uniform distribution of the association weights, all the facilities get allocated at the same spatial coordinates given by (13) and all the corresponding transportation paths are the same. Now as $\beta$ is increased, the simulations show that there is no perceptible change on the facility locations till a critical value of $\beta = \beta_{cr1}$ is reached; beyond which the number of *distinct* facility locations and the number of distinct transportation paths increases. Again as $\beta$ is increased further, there is no change in the facility location and transportation paths till the next critical value of $\beta = \beta_{cr2}$ is reached, where the number of distinct facility locations and transportation paths increases again. These *phase transitions* are of interest as they can help control the number of distinct facilities that one may want to allocate to the network of nodes and also help in speeding up the annealing process.

The critical values of $\beta$ ($\beta_{\text{cr1}}, \beta_{\text{cr2}}, \ldots$) are obtained by tracking the conditions for attaining the minimum of *free-energy* $F$. At $\beta = 0$, the free-energy function is convex, and setting $\frac{\partial F}{\partial y} = 0$ gives the global minimum, also the hessian $\frac{\partial^2 F}{\partial y^2}$ is positive definite. As $\beta$ increases, at a particular $\beta = \beta_{cr1}$, $\frac{\partial F}{\partial y} = 0$ and the Hessian *loses* rank. Here bifurcation occurs leading to an increase in the number of distinct facility locations. Using variational calculus, the necessary condition for $y$ to be a minimum of $F$ requires that for all choices of finite perturbation $\psi$

$$\left.\frac{\partial F_\epsilon}{\partial \epsilon}\right|_{\epsilon=0} = 0, \quad \text{and} \tag{14}$$

$$\left.\frac{\partial^2 F_\epsilon}{\partial \epsilon^2}\right|_{\epsilon=0} = \sum_{\gamma\in\mathcal{G}} p(\gamma)\Lambda_\gamma^T\left(\mathbb{I} - 2\beta\Upsilon_\gamma\right)\Lambda_\gamma + 2\beta\sum_{\gamma_0\in\Gamma_0}\rho_{\gamma_0}\left[\sum_{\gamma\in\mathcal{G}} p(\gamma|\gamma_0)K_\gamma^T\Lambda_\gamma\right]^2 > 0 \tag{15}$$

where $F_\epsilon = F(y + \epsilon\psi)$, $p(\gamma) = \sum_{\gamma_0}\rho(\gamma_0)p(\gamma|\gamma_0)$, $\Upsilon_\gamma = \sum_{\gamma_0} p(\gamma_0|\gamma)K_\gamma K_\gamma^T$ and $\Lambda_\gamma, K_\gamma$ are as defined in the Appendix C. We characterize phase transition as below.

***Theorem 2:*** The critical value of $\beta$ at which the Hessian (15) is no longer positive definite, i.e., it loses rank is given by $\beta_{cr} = \max_\gamma(2\lambda_{\max}(\Upsilon_\gamma))^{-1}$ where $\lambda_{\max}(\Upsilon_\gamma)$ is the largest eigenvalue of the matrix $\Upsilon_\gamma := \sum_{\gamma_0} p(\gamma_0|\gamma)K_\gamma K_\gamma^T$.

See appendix C for proof.

## V. Adding Multiple Capabilities and Constraints to the Problem

In various applications involving spatial networks the overall design goal includes efficient utilization of facilities and the transportation paths. This often corresponds to incorporating several application based constraints on the network topology or on the facilities. In this section, we elucidate the flexibility of our proposed approach in incorporating such constraints.

### A. Restricted Number of Hops

In certain applications it is be beneficial to restrict the path length $q$ of the shortest transportation path as any extra-hop for the commodity may involve associated penalties and overheads such as processing energy cost and time delays. Let $L_{\gamma_0}$ be the given maximum allowable path length (or the number of hops) for a commodity originating at a node $\gamma_0 \in \Gamma_0$. Therefore all the transportation paths $\gamma \in \mathcal{G}$ with path length greater than $L_{\gamma_0}$ become invalid for $\gamma_0$. This constraint enforces that on an optimal transportation path the facility $\gamma_{k+1}$ depends on the facility $\gamma_k$ as well as the originating node $\gamma_0$ which results into the dissociation of the association weight $p(\gamma|\gamma_0)$ as $p(\gamma|\gamma_0) = \prod_{k=0}^{M} p_k(\gamma_{k+1}|\gamma_k, \gamma_0)$. For notational simplicity we denote $p_k(\gamma_{k+1}|\gamma_k, \gamma_0)$ by $p_{k,\gamma_0}$ whenever it is clear from the context. Using the MEP we obtain the association weights $p_{k,\gamma_0}$ as the Gibbs distribution

$$p_{k,\gamma_0} = \left(e^{-\beta d_k}\right)\frac{\sum_{\substack{\sigma_{k+2},\ldots,\sigma_{L_{\gamma_0}} \\ \sigma_{k+1}=\gamma_{k+1}}} e^{-\beta\sum_{t=k+1}^{L_{\gamma_0}} d_t(\sigma_t,\sigma_{t+1})}}{\sum_{\substack{\sigma_{k+1},\ldots,\sigma_{L_{\gamma_0}} \\ \sigma_k=\gamma_k}} e^{-\beta\sum_{t=k}^{L_{\gamma_0}} d_t(\sigma_t,\sigma_{t+1})}} \tag{16}$$

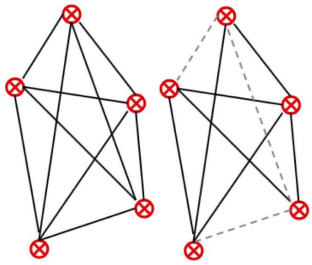

Fig. 3. Fully connected and a partially connected network.

where $\sigma_l \in \Gamma_l \; \forall \; l \in \{k+1, \ldots, L_{\gamma_0}\}$, which when substituted into the expression of $\bar{F}$ in (10) results into

$$F_1 = -\frac{1}{\beta} \sum_{\gamma_0} \rho_{\gamma_0} \log \sum_{\gamma_1, \ldots, \gamma_{L_{\gamma_0}}} e^{-\beta \sum_{t=0}^{L_{\gamma_0}} d_t(\gamma_t, \gamma_{t+1})}. \quad (17)$$

Minimizing (locally) $F_1$ in (17) by setting $\frac{\partial F_1}{\partial y} = 0$, we obtain the facility locations $y$.

### B. Structured (Partially Connected) Network

A transportation link $(f_i, f_j)$ exists (or is active) if a commodity packet is permitted to hop between the facilities $f_i$ and $f_j$.

In a partially connected spatial network, some of the transportation links are absent owing to which the corresponding facility pairs are unable to send across commodities. Fig. 3 demonstrates a fully connected and a partially connected network topology. To incorporate the partial connectivity of the network as a constraint in the optimization problem (3) we introduce a connectivity parameter $\omega_{f_i,f_j}$ defined as

$$\omega_{f_i,f_j} = \begin{cases} 1 & \text{if transportation link } (f_i, f_j) \text{ exists} \\ 0 & \text{otherwise.} \end{cases}$$

We incorporate the connectivity parameter $\omega_{f_j,f_k}$ into the expression of the association weights $p_k(\gamma_{k+1}|\gamma_k)$ (11) in such a manner which assigns $p_k(f_j|f_i) = 0 \; \forall \; k$ for the nonexistent link $(f_i, f_j)$ and rules out all transportation paths that consist of the nonexistent link from the solution space, thus leading to the following expression of the association weights:

$$p_k = \omega_{\gamma_k,\gamma_{k+1}} e^{-\beta d_k} \frac{\sum_{\substack{\sigma_{k+2},\ldots,\sigma_M \\ \sigma_{k+1}=\gamma_{k+1}}} \prod_{t=k+1}^{M} \omega_{\sigma_t \sigma_{t+1}} e^{-\beta d_t}}{\sum_{\substack{\sigma_{k+1},\ldots,\sigma_M \\ \sigma_k=\gamma_k}} \prod_{t=k}^{M} \omega_{\sigma_t \sigma_{t+1}} e^{-\beta d_t}}. \quad (18)$$

We substitute the above association weights into the expression of free energy $\bar{F}$ in (10) to obtain $F_2$, which is then minimized (locally) by setting $\frac{\partial F_2}{\partial y} = 0$ to obtain the facility locations $y$.

### C. Capacity Constraint on Facilities and Path Links

In certain applications, the capacity and cost constraints on the facilities result in corresponding constraints on their usage by transportation paths. For instance, the warehouses $f_j$ in Fig. 1(a) may have limited storage capacity for agricultural goods collected from the farms. The decision variables in our framework appropriately quantify the usage $C(f_j)$ of each facility $f_j$ as

$$C(f_j) = \sum_{\gamma_0} \rho_{\gamma_0} p_0(f_j|n_0) + \sum_{\gamma_0,\gamma_1} \rho_{\gamma_0} p_0(\gamma_1|\gamma_0) p_1(f_j|\gamma_1) + \cdots + \sum_{\gamma_0,\ldots,\gamma_{M-1}} \rho_{\gamma_0} p_0(\gamma_1|\gamma_0) \ldots p_{M-1}(f_j|\gamma_{M-1}) \quad (19)$$

where the first term in the above expression indicates the effective number of transportation paths passing over $f_j$ in the stage $\Gamma_1$, the second term indicates the effective number of paths passing over $f_j$ in the stage $\Gamma_2$, and so on until the last term which indicates the effective number of paths passing over $f_j$ in the last stage $\Gamma_M$. We address the facility capacity constraint by requiring the usage of the facility $f_j$ to be given by $C(f_j) = w_j$, where $w_j$ denotes the predefined capacity of the $j$th facility. The corresponding unconstrained Lagrangian is given by

$$\bar{F}_3 = \bar{F} + \sum_{j=1}^{M} \alpha_{f_j} \left( C(f_j) - w_j \right) \quad (20)$$

where $\bar{F}$ is given in (10). Minimizing $\bar{F}_3$ with respect to the association weights $\{p_k(\gamma_{k+1}|\gamma_k)\}$, we obtain

$$p_k = e^{-\beta(d_k + \alpha_{\gamma_{k+1}})} \frac{\sum_{(\gamma_{k+2},\ldots,\gamma_M)} e^{\sum_{t=k+1}^{M} -\beta(d_t + \alpha_{\gamma_{t+1}})}}{\sum_{(\gamma_{k+1},\ldots,\gamma_M)} e^{\sum_{t=k}^{M} -\beta(d_t + \alpha_{\gamma_{t+1}})}} \quad (21)$$

where $\alpha_{\gamma_k}$ is a Lagrange multiplier in (20). We refer to $\zeta_{\gamma_k} := e^{-\beta \alpha_{\gamma_k}} \forall \gamma_k \in \Gamma_k \backslash \{\delta\}$ as the weight parameter. Substituting (21) in (20) to obtain $F_3$ and minimizing (locally) $F_3$ with respect to $y$ gives the expression for facility locations $y$. To obtain the parameters $\zeta_{f_j}$, we substitute the association weights (21) in the expression (19) of $C(f_j)$ and equate the subsequent expression to $w_j$ (i.e., set $C(f_j) = w_j$). This results in the update equation

$$\zeta_{f_j}^{p+1} = \zeta_{f_j}^{p} \frac{w_j}{C(f_j)}, \forall j \in \{1, 2, \ldots, M\}. \quad (22)$$

In our algorithm, we minimize the *free-energy* $\bar{F}_3$ at successively increasing values of $\beta$ by alternating between the expressions of association weights in (21), facility locations $y$, and the update equation for $\zeta_{f_j}$ in (22).

Similarly, in certain application areas, the amount of traffic $\eta_{f_i f_j}$ that a transportation link $(f_i, f_j)$ is able to handle is known *a priori*. Using the decision variables in our framework we appropriately quantify the usage $C_{f_i f_j}$ of each transportation link from $f_i$ to $f_j$ as

$$C_{f_i f_j} = p_1(f_j|f_i) \sum_{\gamma_0} \rho_{\gamma_0} p_0(f_i|\gamma_0) + p_2(f_j|f_i) \sum_{\gamma_0,\gamma_1} \rho_{\gamma_0} p_0(\gamma_1|\gamma_0) p_1(f_i|\gamma_1) + \cdots + p_{M-1}(f_j|f_i) \sum_{\gamma_0,\ldots,\gamma_{M-2}} \rho_{\gamma_0} p_0(\gamma_1|\gamma_0) \cdots p_{M-2}(f_i|\gamma_{M-2}) \quad (23)$$

where the first term in the above expression is the fraction of total paths with node $f_i \in \Gamma_1$ and $f_j \in \Gamma_2$, i.e., the fraction of

paths with $(f_i, f_j)$ transportation link occurring in the hop from stage $\Gamma_1$ to stage $\Gamma_2$. Similarly, the other subsequent terms count the fraction of the transportation paths with $(f_i, f_j)$ link in the hop from stage $\Gamma_k$ to $\Gamma_{k+1}$ for all $k \in \{2, \ldots, M-1\}$. The unconstrained Lagrangian in this case is given by

$$\bar{F}_4 = \bar{F} + \sum_{i,j:i\neq j} \alpha_{f_i f_j} \left( C_{f_i f_j} - \eta_{f_i f_j} \right) \tag{24}$$

where $\bar{F}$ is given by (10). The association weights $\{p_k(\gamma_{k+1}|\gamma_k)\}$ that minimize $\bar{F}_4$ are given by

$$p_k = e^{-\beta(d_k + \alpha_{\gamma_k \gamma_{k+1}})} \frac{\sum_{(\gamma_{k+2},\ldots,\gamma_M)} e^{\sum_{t=k+1}^{M} -\beta(d_t + \alpha_{\gamma_t,\gamma_{t+1}})}}{\sum_{(\gamma_{k+1},\ldots,\gamma_M)} e^{\sum_{t=k}^{M} -\beta(d_t + \alpha_{\gamma_t,\gamma_{t+1}})}} \tag{25}$$

where $\lambda_{\gamma_k \gamma_{k+1}} := e^{-\beta \alpha_{\gamma_k \gamma_{k+1}}} \forall \gamma_k, \gamma_{k+1}$ is referred to as the weight parameter. Substituting (25) in the expression of *free-energy* $\bar{F}_4$ (24) to obtain $F_4$ and setting $\frac{\partial F_4}{\partial y} = 0$ gives the facility locations $y$. To obtain the parameters $\lambda_{f_i f_j}$, we substitute the association weights (25) in the expression (23) of $C_{f_i f_j}$ and equate the subsequent expression to $\eta_{f_i f_j}$ (i.e., set $C_{f_i f_j} = \eta_{f_i f_j}$). This results in the update equation

$$\lambda_{f_i f_j}^{p+1} = \lambda_{f_i f_j}^{p} \frac{\eta_{f_i f_j}}{C_{f_i f_j}}. \tag{26}$$

As before, our algorithm minimizes *free-energy* $\bar{F}_4$ at successively increasing values of $\beta$ by alternating between the expressions of the association weights (25), facility locations $y$ and the update equation for $\lambda_{f_i f_j}$ in (26).

## VI. Extension to Dynamic Spatial Networks

In the case of dynamic spatial networks, the nodes and the destination center have an associated dynamics given by continuously differentiable velocity fields $\phi_i(x_i(t), t) \in \mathbb{R}^d$, $1 \leq i \leq N$ and $\psi(z(t), t) \in \mathbb{R}^d$, respectively. The resulting facility locations and the transportation paths are also time varying and the entire dynamical system is represented as

$$\dot{\zeta} = f(\zeta(t), t) \Longleftrightarrow \begin{cases} \dot{x}(t) &= \Phi(x(t), t) \\ \dot{z}(t) &= \Psi(z(t), t) \\ \dot{y}(t) &= u(x(t), z(t), y(t), t) \end{cases} \tag{27}$$

where $x(t) = [x_1^T(t), \ldots, x_N^T(t)]^T \in \mathbb{R}^{Nd}$, $\Phi = [\phi_1^T(t), \ldots, \phi_N^T(t)]^T \in \mathbb{R}^{Nd}$, $u(t) = [u_1^T(t), \ldots, u_M^T(t)]^T \in \mathbb{R}^{Md}$, and $\zeta(t) = [x(t)^T, z(t)^T, y(t)^T]^T \in \mathbb{R}^{(N+1+M)d}$.

Similar to the static spatial networks, the problem of simultaneous facility location and path optimization in dynamic spatial networks ($d$-FLPO) has twofold objectives: 1) allocate facilities $y_j(t)$, $1 \leq j \leq M$ in the domain $\Omega$; 2) design optimal transportation path from each node $n_i$ to the destination center $\delta$ such that the cost function (3) gets minimized at every time instant $t$.

A straightforward approach to solve the $d$-FLPO problem is to solve the $s$-FLPO problem at every time instant to determine the facility locations and the transportation paths. However, it is quite evident that such a methodology is computationally expensive. A specific shortcoming of this method is that it does not employ the past knowledge of facility locations and transportation routes to determine the solution at current time instant, which may potentially lead to big changes (jumps) in facility locations over a very small time intervals; and may not be practically achievable as shown in Section VII.

We propose a control-based framework to solve the $d$-FLPO problem that builds upon the solution of the $s$-FLPO problem obtained at the initial time instant $t_0$. In our framework, we use the free-energy function $F$ (12) as a Lyapunov candidate function for the dynamical system (27) and design the control for facility dynamics $\dot{y}(t) = u(t)$ such that $\dot{F} \leq 0 \, \forall \, t \geq 0$. Note that $F$ is a smooth approximation of $D$ in (7) which incorporates cost functions for both facility location and path optimization problems. Once the dynamics of the facilities are known, the time-varying transportation paths can be deduced from (11). The following theorem justifies the choice of free-energy $F$ as a Lyapunov function.

***Theorem 3:*** Let $F$ be the free-energy function (12) corresponding to the dynamical system (27) then

a) $F(\zeta) + \frac{1}{\beta} \log |\mathcal{G}| > 0 \;\; \forall \zeta = [x^T, y^T, d^T]^T \in \mathbb{R}^{(N+M+1)d}$ where $\mathcal{G} = \{(\gamma_1, \ldots, \gamma_M) : \gamma_k \in \Gamma_k \forall 1 \leq k \leq M\}$ is the set of all possible paths when $M$ facilities are allocated.

b) The derivative

$$\frac{\partial F}{\partial \zeta} = \begin{bmatrix} \hat{P}_{\gamma_0} & -\hat{P}^0(\gamma_1, \gamma_0) & 0 \\ -\hat{P}^0(\gamma_1, \gamma_0)^T & 2\hat{A} - \hat{B} & -\hat{C} \\ 0 & -\hat{C}^T & I \end{bmatrix} \tag{28}$$

is a symmetric matrix, where $\hat{P}_{\gamma_0} = I_d \otimes P_{\gamma_0}$, $P_{\gamma_0} = \text{diag}(\{\rho_{\gamma_0}\})$, $\hat{P}_0(\gamma_1, \gamma_0) = I_d \otimes P_0(\gamma_1, \gamma_0)$, $P_0(\gamma_1, \gamma_0) = [p_{\gamma_0} p_0(\gamma_1|\gamma_0)]$ and $I_d$ is an identity matrix of size $d \times d$. Also note that $\dot{F}(t) = 2\zeta^T \frac{\partial F}{\partial \zeta} \dot{\zeta}$.

c) There is no dynamic control authority at the facility locations $y_c(t) = (2\hat{A} - \hat{B})^{-1}(\hat{X} + \hat{C})$ obtained in (13), i.e., $\frac{\partial \dot{F}}{\partial u} = 0$ at $y(t) = y_c(t)$.

Please refer the Appendix D for proof of the above theorem. The facilities are at the positions $y_c(t)$ (13) only when $\bar{y}(t) := y(t) - y_c(t) = 0$. We transform the coordinates $\zeta = [x^T, y^T, z^T]^T$ to $\bar{\zeta} = [x^T, \bar{y}^T, z^T]^T$, where $\bar{y} = y - y_c$. In the new coordinates, the dynamics of the facility locations are given by

$$\begin{aligned} \dot{\bar{y}}(t) = \bar{u}(t) - (2\hat{A} - \hat{B})^{-1} \Big[ &(2\dot{\hat{A}} - \dot{\hat{B}}) y_c \\ &+ \dot{\hat{P}}^0(\gamma_1, \gamma_0)^T x + \dot{\hat{C}} z \Big] \end{aligned} \tag{29}$$

where $\bar{u} = u - (2\hat{A} - \hat{B})^{-1}(\hat{P}^0(\gamma_1|\gamma_0)^T \Phi + \hat{C}\Psi)$ and

$$\begin{aligned} \dot{F} = &(x^T \hat{P}_{\gamma_0} - y_c^T \hat{P}_0(\gamma_1|\gamma_0)^T)\Phi \\ &+ [z^T - y_c^T \hat{C}]\psi + \bar{y}^T (2\hat{A} - \hat{B})\bar{u}(t). \end{aligned} \tag{30}$$

We take advantage of the affine dependence of $\dot{F}$ on $\bar{u}(t)$ in (30) to determine the choice of $\bar{u}(t)$ such that $\dot{F} \leq 0$ [35]–[37]. More particularly, we choose control

$$\bar{u}(\bar{\zeta}) = -\left[ K_0 + \frac{\alpha + \sqrt{|\alpha|^2 + (\bar{y}(2\hat{A} - \hat{B})\bar{y})^2}}{\bar{y}^T (2\hat{A} - \hat{B})\bar{y}} \right] \bar{y} \tag{31}$$

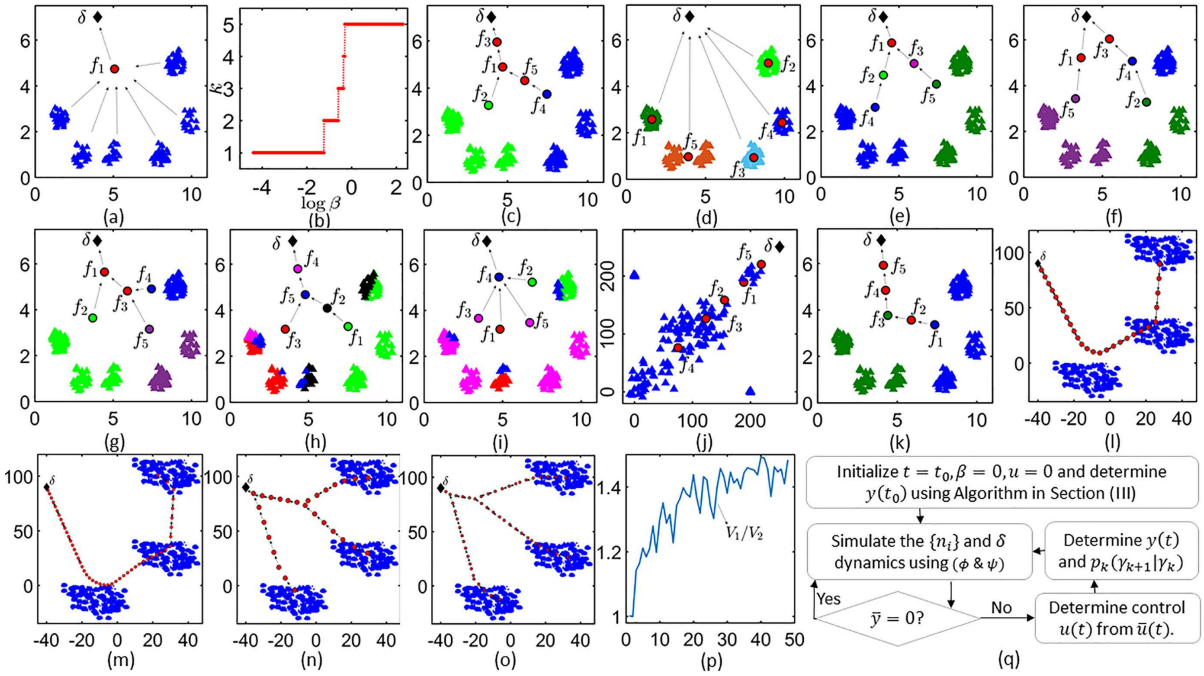


Fig. 4. Nodes, facilities, and the destination center are represented by triangles, circles and diamond, respectively. (a) At $\beta \approx 0$ all facilities are coincident. (b) Phase transition phenomenon. (c) Facility locations and paths at $\beta \to \infty$. The first facility to each node is colored identically to that node. The commodity hops to the subsequent facilities from the first facility as denoted by the arrows. (d) Two-step methodology for *s*-RARO. (e) Illustrates *s*-FLPO where $L_{\gamma_0} = 3\ \forall \gamma_0 \in \Gamma_0$. (f) Partially connected network - pairs $(f_1, f_2)$, $(f_4, f_1)$, $(f_2, f_3)$, $(f_4, f_5)$ and $(f_5, f_3)$ do not exist. (g) Facility capacity constraint $w_1 : w_2 : w_3 : w_4 : w_5 = 4 : 2 : 2 : 1 : 1$. (h) Facilities constrained as entry facilities in proportion 4:2:2.5:0.1:1.0 (i) Transportation link capacity constraints $\eta_{f_1 f_4} : \eta_{f_2 f_4} : \eta_{f_3, f_4} : \eta_{f_5, f_4} = 0.3 : 0.7 : 1 : 1$; all other communication links have zero capacities. (j) For comparing computation times with [28]. Our algorithm - 1.85s, algorithm in [28] - 24.86s. (k) Solution using framework from [29]. (l)–(m) Large scale problem with $N = 17028$, $M = 27$ and $M = 50$ in (l) and (m), respectively. Solved using the algorithm in [29]. (n) and (o) Large scale problem with $N = 17028$, $M = 27$ and $M = 50$ in (n) and (o), respectively. Solved using the algorithm in the current work. (p) Comparing the objective function value ($V_1/V_2$) at various number of facilities $M$ as given by algorithm in [29] ($V_1$) and our current work ($V_2$) for the previous large scale setting of nodes and destination. (q) Flowchart of the proposed algorithm in the *d*-FLPO problem.

where $\bar{y} \neq 0$, $K_0 > 0$ and $\alpha = (x^T \hat{P}_{\gamma_0} - y_c^T \hat{P}_0(\gamma_1|\gamma_0)^T)\Phi + [z^T - y_c^T \hat{C}]\psi$. The following two theorems establish that the facility locations $y(t)$ converge asymptotically to $y_c(t)$ and the control effort (31) is bounded near $\bar{y} = 0$.

***Theorem 4:*** Asymptotic convergence: For the dynamical system (27) the choice of control $\bar{u}(\bar{\zeta})$ in (31) results in $\dot{F} \leq 0$ $\forall\ t \geq 0$ and $\bar{y}(t) \to 0$ as $t \to \infty$.

***Theorem 5:*** Lipschitz continuity: If there exists a control $\hat{\bar{u}} : \mathbb{R}^{(N+M+1)d} \to \mathbb{R}^{Md}$ Lipschitz at $\bar{\zeta} = 0$ such that $\dot{F} \leq 0\ \forall\ t \geq 0$ for $\bar{u} = \hat{\bar{u}}$, then the choice of control $\bar{u}$ in (31) is Lipschitz at $\bar{\zeta} = 0$. That is, $\exists\ \epsilon > 0$ and a constant $c_0$ such that $\|\bar{u}(\bar{\zeta})\| \leq c_o \|\bar{\zeta}\|$ for $\|\bar{\zeta}\| \leq \epsilon$.

Please refer to the Appendix D for the proof of the above two theorems. *Remarks:* 1) The above control design methodology can be extended to the *d*-FLPO problems with additional constraints over the network topology and facilities. In fact, our simulations in Section VII demonstrate the *d*-FLPO problem where the spatial network is partially connected. 2) Theorem 5 emphasizes the nonconversativeness of our solution; i.e., if there exists a Lipschitz (bounded) solution such that $\dot{F} \leq 0$ then Theorem 5 implies that our proposed solution is also Lipschitz (bounded). 3) For the purpose of simulation, we discretize time into $\Delta t$ intervals. At instants $\bar{y} \neq 0$ we determine the dynamics of $y(t)$ using $\bar{u}$ in (31). This results into $\dot{F} \leq 0$ at all such time instants. For the time instants when $\bar{y} = 0$ we already have the facilities at the locations $y_c$. At such instants $\dot{F}$ may be positive, negative or zero depending on the dynamics of the node and the destination center.

## VII. Simulation and Results

In this section, we simulate our proposed algorithms for the *s*-FLPO and *d*-FLPO problems. We first illustrate the *s*-FLPO problem. For the purpose of simulations we randomly distribute 200 nodes around 6 randomly chosen points in an $11 \times 8$ square unit area. The location of the destination (marked as $\delta$) is randomly chosen to be at $(4, 7)$. For the purpose of illustration we assume the cost function $d_k(\cdot, \cdot)$ to be squared-euclidean distance. Consider the scenario where we allocate $M = 5$ facilities. As stated in Section IV, at low value of $\beta$, all the facilities $\{f_j\}_{j=1}^5$ get allocated at the same spatial coordinates as shown in Fig. 4(a), where the triangles denotes the nodes, circle denotes the facilities and the diamond denotes the destination. As the value of $\beta$ increases the number of distinct facility locations increases [see Fig. 4(b)], and the final facility locations and transportation paths are obtained as $\beta$ becomes sufficiently large

as shown in Fig. 4(c). In Fig. 4(c), a node of a particular color first sends its commodity packet to the facility of the similar color which then reaches the destination center via the path indicated in the figure. Observe that in Fig. 4(c) all the nodes $\gamma_0$ either opt for the 4-hop path $f_4 \to f_5 \to f_1 \to f_3 \to \delta$ or the 3-hop path $f_2 \to f_1 \to f_3 \to \delta$. The total cost of transportation incurred is 12.58 units. Fig. 4(d) illustrates the solution to the same problem using the sequential approach illustrated in Section III which incurs a total transportation cost of 34.16 units, 2.7 times the cost incurred in Fig. 4(c). This demonstrates that the sequential approach results into a solution with a much higher cost as compared to the simultaneous approach.

*Restricted Number of Hops:* Fig. 4(e) illustrates the solution to the *s*-FLPO problem when the maximum path length is restricted to 3 for all the nodes, i.e. $L_{\gamma_0} = 3 \; \forall \; \gamma_0 \in \Gamma_0$. Observe that now all the nodes opt for either $f_4 \to f_2 \to f_1 \to \delta$ or $f_5 \to f_3 \to f_1 \to \delta$ paths, both of which have path length of 3. The total cost in this case is 12.71 units, which is approximately 1% higher than the scenario in Fig. 4(c) where there is no restriction on the maximum path length. We can deduce the effectiveness of restricting hops to 3 which only leads to about 1% cost increase; that is marginal utility of adding more hops is only about 1%.

*Partially Connected Network:* Fig. 4(f) simulates a partially connected spatial network. For the purpose of simulation, we assume that the transportation links $(f_1, f_2)$, $(f_2, f_3)$, $(f_4, f_1)$, $(f_1, f_3)$, $(f_4, f_5)$, and $(f_5, f_3)$ are absent. As shown in the figure, the algorithm respects the constraint posed by the partially connected network and assigns the facility locations and paths correspondingly. The total cost of transportation is 12.92 units. Note the difference with the facility location and transportation path assignments in a fully connected network Fig. 4(c).

*Capacity Constraints:* Fig. 4(g) demonstrates the capacity constraints on various facilities. Here, facility capacities are distributed as $w_1 : w_2 : w_3 : w_4 : w_5 = 4 : 2 : 2 : 1 : 1$. In the figure, the final facility allocation and path design is in such a way that $C(f_1) : C(f_2) : C(f_3) : C(f_4) : C(f_5) = 3.85 : 1.75 : 2.10 : 1 : 1.1$ which is approximately as given in the constraint. The slight mismatch in the values of the usage $C(f_j)$ and capacities $w_j$ could be because of numerical issues in MATLAB and we are currently looking into it. Similarly, Fig. 4(h) demonstrates the scenario when the facilities are constrained in their capacity to act as an entry facility of a node in the proportion $4 : 2 : 2.5 : 0.5 : 1.0$. The final solution is such that a proportion $3.9 : 1.9 : 2.5 : 0.5 : 1.0$ is achieved for the facilities as the entry point for the nodes in the network. Note the color changes for the nodes in comparison to Fig. 4(c), (f), and (g). Fig. 4(i) illustrates the scenario when the capacities of the transportation links are known *a priori*. We assume that all the transportation links except $(f_1, f_3), (f_2, f_3)$, $(f_3, f_4)$ and $(f_5, f_4)$ have zero capacities and we constrain that $\eta_{f_1 f_4} : \eta_{f_2 f_4} : \eta_{f_3 f_4} : \eta_{f_5 f_4} = 3 : 7 : 10 : 10$. Upon simulation, the facilities are allocated and transportation paths are fixed in such a way that the $C_{f_1 f_4} : C_{f_2 f_4} : C_{f_3 f_4} : C_{f_5 f_4} = 3.3 : 6.3 : 9 : 9$, i.e., the solution given by the algorithm complies with the constraint on the communication link capacities. The total cost of communication is 15.8 units.

*Comparison With Previous Works:* Next we compare our proposed method with [28] and [29]. We begin with comparing the computation time of the algorithm presented in this article with the one proposed in [28]. The computation time for the problem setting shown in Fig. 4(j) is 24.86 s, while the algorithm presented in this article takes 1.85 s which is just 8% of the former. Note that the [28] uses MATLAB to run the algorithm on an Intel Core 2 Duo T5470 1.6-GHz processor with 2-GB RAM, while we used MATLAB to code and run our algorithm on i3 2.3-GHz processor with 2-GB RAM. We note that the improvement in the computation time comes from the scalability of the algorithm proposed in this article, since the configuration of the two machines used are almost similar. Fig. 4(k) demonstrates the solution to the *s*-FLPO problem as given by the algorithm in [29]. Here, the total cost of transportation comes out to be 14.93, which is 18% (or 2.35 units) more than the solution Fig. 4(c) given by the algorithm presented in this article.

*Large Scale Problems:* Fig. 4(l)–(o) demonstrate a large scale *s*-FLPO problem setting with $N = 17\,028$ nodes as indicated by the blue triangles. In Fig. 4(l) and (n), we allocate $M = 27$ facilities using the algorithm in [29] and our current work, respectively. Note the qualitative difference between the two solutions where the allocated facilities and the transportation paths resulting from the latter are more distributed in the domain as compared to [29]. The objective function value for the solution in Fig. 4(l) is 1323.07 units and for Fig. 4(n) is 985.87 units; which is a improvement of 25% over the former. Similarly, in Fig. 4(m) and (o) we allocated $M = 50$ facilities using the approach in [29] and our current algorithm, respectively. The objective value for the solution in Fig. 4(m) is 864.35 and for the solution in Fig. 4(n) is 582.70; approximately 33% lesser objective function value is obtained using our current framework. The above quantifies the fact that the framework developed in [29] results into suboptimal solutions as compared to our current framework when applied to a general *s*-FLPO problem. Also note that the framework presented in [28] is computationally intractable for both the above cases of $M = 27$ and $M = 50$ facilities as it requires $2.9 \times 10^{28}$ and $8.2 \times 10^{64}$ many decision variables, respectively; the corresponding memory requirements are unthinkable. Fig. 4(p) compares the cost function value of the solutions obtained using [29] ($V_1$) and our current work ($V_2$) for various number of facilities $M$ allocated in the large scale setting of nodes and destination illustrated in Fig. 4(l)–(o). Note that the ratio $\eta = V_1/V_2 (> 1)$ increases with number of allocated facilities and reaches close to 1.5 (i.e., 50% increase in the cost function values in [29]) for values of $M \gtrapprox 40$—clearly indicating suboptimality of the framework [29] when applied to general *s*-FLPO problem setting.

*d-FLPO in Partially Connected Network:* We consider the scenario of partially connected spatial network where the transportation links $(f_1, f_2)$, $(f_2, f_3)$, $(f_4, f_1)$, $(f_1, f_3)$, $(f_4, f_5)$, and $(f_5, f_3)$ are absent. The main steps of the algorithm are summarized in Fig. 4(q). The sequence of images in Fig. 5 (a1)–(a4) demonstrate the dynamics of the facilities and the transportation paths for randomly chosen dynamics of the nodes and the destination center. The node and destination center dynamics are simulated for a total duration of 20 s and the dynamics of the facilities and transportation paths are determined using (31) after every time interval of $\Delta t = 0.03$ s. Observe the change in the *entry facility* of the nodes (marked by the change

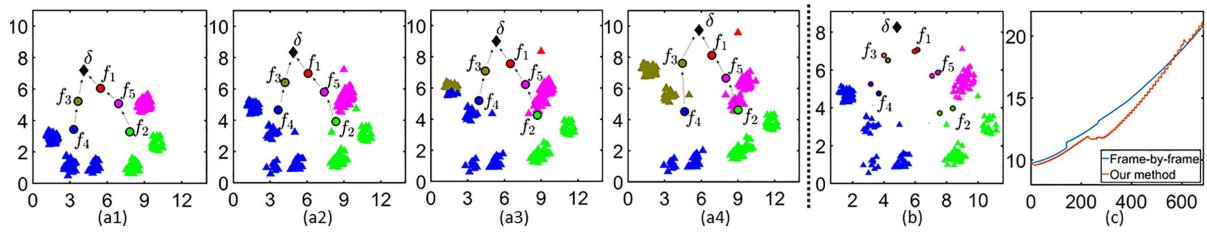


Fig. 5. (a1)–(a4) Solution to the *d*-FLPO problem. Observe the change in spatial coordinates of the nodes, destination center and the facilities. Also, observe the change in the color of the triangles from (a2) to (a3) and (a3) to (a4), indicating the change in their transportation paths. (b) Nonviable dynamics of the facility locations. Observe the considerable change in spatial location of $f_2$ and $f_4$ over a small interval of 0.03 s. (c) Comparing distortion from the two approaches.

in their color) and their corresponding transportation path in Fig. 5(a1)–(a4).

The *frame-by-frame* approach takes approximately 700 times more computational time than our approach for the example considered above. Fig. 5(c) compares the distortion $D_0$ obtained from our control-based approach and the frame-by-frame solution. Apart from that, the simulations using frame-by-frame approach show sudden jumps in positions which may be impractical for scenarios with bounded velocities, for instance in Fig. 5(b), note the sudden jump in positions of facilities $f_2$ and $f_4$ in the span of two time instants that are only 0.03 s apart.

## VIII. Analysis and Discussion

### A. Flexibility of the Framework

The proposed framework is flexible to incorporate various additional constraints on the *s*-FLPO and *d*-FLPO problems in terms of the network topology, facilities, or the transportation paths as illustrated in Section V. Our framework also generalizes to different choices of distance functions $d_k(\gamma_k, \gamma_{k+1})$ as against the squared euclidean function considered in this article.

### B. Robustness Analysis

The solutions obtained to *s*-FLPO and *d*-FLPO problems are sensitive to various attributes of the nodes and the destination center (such as spatial locations, dynamics, and distance cost functions). This necessitates a study to classify such attributes, that affect the final solution, into various categories of importance. Our framework easily facilitates such a study through the free energy function $F$ which is a smooth approximation of the cost function $D$. For instance, the derivatives $\frac{\partial F}{\partial x_i}$, $\frac{\partial F}{\partial y_j}$, and $\frac{\partial F}{\partial d}$ measure the sensitivity of the final solution to the spatial location of the node $n_i$, facility $f_j$, and destination $\delta$, respectively.

### C. Uncertainty in Parameters

In certain applications, instead of the exact information about various attributes of the nodes and the destination centre, a partial knowledge in terms of distributions of these attributes may be known. For instance, instead of the exact spatial location $x_i$ of the node $n_i$, distribution $p(x_i|n_i)$ for the spatial location is known. Our proposed framework easily incorporates such uncertainties in parameter values. For example, the above uncertainty in the spatial locations of the nodes will result into replacing $d(n_i, f_j)$ with $d'(n_i, f_j) = \sum_{x_i} p(x_i|n_i) d(n_i, f_j)$ and the remainder of the problem solution follows as in Section III.

*D. Application to Parameterized Finite Horizon Markov Decision Processes (MDPs):* The stage-wise framework proposed in Fig. 2 facilitates a viewpoint where in our MEP-based solution approach for the FLPO problem is easily extendable to the class of sequential decision making problems that are modeled as finite horizon MDPs with *parameterized* state space. In particular, consider the MDP given by $\mathcal{M} = \langle \mathcal{S}, \mathcal{A}, c, \mathcal{P}, H \rangle$ where $\mathcal{S}$ is the state space, $\zeta(s)$ for $s \in \mathcal{S}$ represents the unknown parameter (e.g., facility locations in FLPO), $\mathcal{A}$, $c : \mathcal{S} \times \mathcal{A} \to \mathbb{R}$, $\mathcal{P} : \mathcal{S} \times \mathcal{S} \times \mathcal{A} \to \{0, 1\}$, and $H$, respectively, denote the set of actions, the cost function, the state transition probability, and maximum number of stages. The underlying FLPO-type objective is to $\min_{\{\zeta(s)\}, \{\mu_t(s)\}} J := \sum_{s \in \mathcal{S}} \rho(s) J(s)$ where

$$J(s) = \sum_{\mathcal{X}} \bar{p}_\mu(\mathcal{X}|x_0 = s) \left[ \sum_{t=0}^{H} c(x_t, \mu_t(x_t)) \right] \tag{32}$$

$\rho(s)$ denotes the weight of each state $s \in \mathcal{S}$, $\mu_t(\cdot)$ is the policy under which the state $x_t = s \in \mathcal{S}$ is followed by $x_{t+1} = \mu_t(s) \in \mathcal{S}$, $\mathcal{X} := (x_0, x_1, \ldots, x_H)$ denotes a sequences of states and $\bar{p}_\mu(\cdot|s)$ is the distribution over the space of all possible sequences $\mathcal{X}$. Note the resemblance of the objective function here with the cost function $D$ in (5) of the FLPO problem where the unknown parameters $\zeta(s)$ are the facility locations $\{y_j\}$ and the policy $\mu_t(\cdot)$ is analogous to the association weights $\{p_k(\cdot|\cdot)\}$. Hence, the solution methodology detailed out in Section III also solves the optimization problem posed by the parameterized finite horizon MDPs.

## Appendix A

Definitions of matrices in the expression of $y$ in (13)

1) $A = \sum_{i=1}^{M} A_i$, where $A_i \in \mathbb{R}^{M \times M}$ is a diagonal matrix such that $(A_i)_{jj} = \sum_{\gamma_0, \gamma_1, \ldots, \gamma_{i-1}} \rho_{\gamma_0} p_0(\gamma_1|\gamma_0) \ldots p_{i-1}(f_j|\gamma_{i-1})$.
2) $B = \sum_{i=1}^{M-1} (B_i + B_i^T)$ where $B_i \in \mathbb{R}^{M \times M}$ is such that $(B_i)_{mn} = \sum_{\gamma_0, \gamma_1, \ldots, \gamma_{i-1}} \rho_{\gamma_0} p_0(\gamma_1|\gamma_0) \ldots p_{i-1}(f_m|\gamma_{i-1}) p_i(f_n|f_m)$.
3) $\bar{X} \in \mathbb{R}^{M \times n}$, where $\bar{X}_{mn} = \sum_{\gamma_0} \rho_{\gamma_0} p^0(f_m|\gamma_0)(\xi(\gamma_0))_n$, and $(\xi(\gamma_0))_n$ is the $n$th component of the spatial coordinate of $\gamma_0$.
4) $C = \bar{B} + \sum_{i=2}^{M-1} \tilde{B}_i + \sum_{j=2}^{M-1} \check{B}_j + \bar{D} \in \mathbb{R}^{M \times n}$, where $(\bar{B})_{mn} = \sum_{\gamma_0} \rho_{\gamma_0} p_0(f_m|\gamma_0) p_1(\delta|f_m) z_n$,

$(\tilde{B}_i)_{mn} = \sum_{\gamma_0,\gamma_1,\ldots,\gamma_{i-1}} \rho_{\gamma_0} p_0 \ldots p_{i-2} p_{i-1}(f_m|\gamma_{i-1})$ $p_i(\delta|f_m) z_n$,
$(\check{B}_i)_{mn} = \sum_{\gamma_0,\gamma_1,\ldots,\gamma_{i-1}} \rho_{\gamma_0} p_0 \ldots p_{i-2} p_{i-1}(\delta|\gamma_{i-1}) p_i$ $(f_m|\delta) z_n$,
$(\bar{D})_{mn} = \sum_{\gamma_0,\ldots,\gamma_{M-1}} \rho_{\gamma_0} p_0 \ldots p_{M-1}(f_m|\gamma_{M-1}) z_n$,
and $z_n$ denotes the $n$th coordinate of the destination $\delta$.

The matrix $C := 2\hat{A} - \hat{B}$ is such that for every $i$th row in $C$ the sum of absolute value of the off-diagonal entries ($\sum_{j\neq i} |[C]_{ij}|$) is less than the absolute value of the diagonal element ($|[C]_{ii}|$) in that row, i.e. $\sum_{j\neq i} |[C]_{ij}| < |[C]_{ii}|$. Thus, by Gerhgorin's circle theorem [38], all the eigenvalues of $C$ are positive and hence $C$ is a positive definite matrix.

## APPENDIX B

*Proof of Theorem 1:* As indicated in the algorithm, at each value of the annealing parameter $\beta_t$, where $t$ denotes the $t$th iteration, it is required to solve the following implicit equation iteratively $y = (2\hat{A}(y) - \hat{B}(y))^{-1}(\hat{\bar{X}}(y) + \hat{C}(y))$. The corresponding iteration scheme (where $n$ denotes the iterate number) solves for $y_t$ at each value of $\beta_t$

$$y_t(n+1) = \underbrace{(2\hat{A}_t(n) - \hat{B}_t(n))^{-1}(\hat{\bar{X}}_t(n) + \hat{C}_t(n))}_{=:G_t(y_t(n))}$$

where $\hat{A}_t(n), \hat{B}_t(n), \hat{\bar{X}}_t(n)$ and $\hat{C}_t(n)$ are dependent on $y_t(n)$. The *free-energy* at the $n$th iteration for the annealing parameter $\beta_t$ is given by $F_t(n) = -\frac{1}{\beta_t} \sum_{\gamma_0\in\mathcal{S}} \rho_{\gamma_0} \log \sum_{\gamma\in\mathcal{G}} e^{-\beta_t \sum_{t=0}^{M} d_t(\gamma_t(n),\gamma_{t+1}(n))}$ whose gradient with respect to $y$ is $\nabla F_t(n) = 2(2\hat{A}_t(n) - \hat{B}_t(n))(y_t(n) - y_t(n+1))$

$$\Rightarrow y_t(n+1) = y_t(n) - \frac{1}{2}(2\hat{A}_t(n) - \hat{B}_t(n))^{-1} \nabla F_t(n),$$

which is of the form $y_t(n+1) = y_t(n) + \alpha_k \chi_t(n)$, where $\chi_t(n) = -(2(A_t(n) - B_t(n))^{-1} \nabla F_t(n)$. The matrix $C_t(n) = (2A_t(n) - B_t(n)) \in \mathbb{R}^{M\times M}$ for every iteration $n$ is such that, for every $i$th row in $C_t$ the sum of absolute value of off-diagonal entries ($\sum_{j\neq i} |(C_t)_{ij}|$) is less than the absolute value of the diagonal element ($|(C_t)_{ii}|$) in that row, i.e. $\sum_{j\neq i} |(C_t)_{ij}| < |(C_t)_{ii}|$. Thus, by Gerhgorin's circle theorem [38], all the eigenvalues of $C_t(n)$ are positive. Hence, $(C_t(n))^{-1}$ is positive definite and the descent direction $\chi_t(n)$ is such that $\chi_t(n)^T \nabla F_t(n) \leq 0$, where the equality holds true only for the case when $\nabla F_t(n) = 0$. Therefore, $\chi_t(n)$ is the descent direction and the current iteration scheme is a descent method which guarantees convergence to a local minimum.

## APPENDIX C

*Definitions of $\Lambda_\gamma$, $K_\gamma$:* $\Lambda_\gamma, K_\gamma \in \mathbb{R}^{M+1}$, $[\Lambda_\gamma]_n = \psi_n - \psi_{n-1}$, $[K_\gamma]_n = \xi(\gamma_n) - \xi(\gamma_{n-1})$, $\mathbb{I} \in \mathbb{R}^{(M+1)\times(M+1)}$ is an identity matrix, $\xi(\gamma_k)$ is the spatial coordinate of $\gamma_k$, $0 \leq k \leq M+1$.

*Proof of Theorem 2:* The solution $y$ to (13) no longer implies a (local) minimum to the cost function as soon as the second order condition in (15) fails. There exists a direction $\psi$ along which the cost can decrease, thereby implying that $y$ is not the minimum. In fact, perturbation of $y$ at such critical $\beta$ and resolving (13) results in a new solution $y$. (as done in step 4 of the annealing algorithm), which has more number of distinct locations $\{y_j\}$. To obtain this critical value of $\beta$, we compute $\frac{\partial^2 F}{\partial \epsilon^2}$ as in (15). We claim that the expression of hessian $\frac{\partial^2 F}{\partial \epsilon^2}$ in (15) is non-negative for all finite perturbation $\psi$ if and only if the matrix $[\mathbb{I} - 2\beta\Upsilon_\gamma]$ is positive definite. The "If" part is straightforward since the second term in the expression is non-negative. For the "only If" part we show that when $[\mathbb{I} - 2\beta\Upsilon_\gamma]$ is not positive definite, there exists a finite perturbation $\psi$ such that the second term becomes zero thereby making the entire expression in (15) negative. Let us assume that there exists a transportation path $\gamma \in \mathcal{G}$ with positive probability such that the matrix $[\mathbb{I} - 2\beta\Upsilon_\gamma]$ is not positive definite. In fact, we assume there are several coincident facilities which result into several coincident transportation paths $\gamma \in \mathcal{G}$ such that $[\mathbb{I} - 2\beta\Upsilon_\gamma]$ is not positive definite. Under such circumstances we see that for the finite perturbation $\Lambda_\gamma = 0 \ \forall\ \gamma \neq \hat{\gamma}$ and $\sum_{\gamma\in\mathcal{G}:\gamma=\hat{\gamma}} \Lambda_\gamma = 0$, the second term in (15) is zero. Thus, whenever the first term in (15) is not positive definite we can construct the above perturbation such that the second term vanishes. Hence the positivity of the expression in (15) for all finite perturbations $\psi$ depends solely on the positive definiteness of $[\mathbb{I} - 2\beta\Upsilon_\gamma]$. The phase transition occurs when the matrix $[\mathbb{I} - 2\beta\Upsilon_\gamma]$ loses its positive definiteness; i.e., $\det[\mathbb{I} - 2\beta\Upsilon_\gamma] = 0 \Rightarrow \beta_{cr}(\gamma) = \frac{1}{2\lambda_{max}(\gamma)}$ where $\lambda_{max}$ is the largest eigenvalue of $\Upsilon_\gamma$. We consider the $\beta_{cr} = \max_\gamma \beta_{cr}(\gamma)$ as we anneal $\beta$ from a large value to zero. The above derivation is analogous to the DA algorithm in [22].

## APPENDIX D

### A. Theorem 3

Part (a), we note that $e^{-\beta \sum_{t=0}^{M} d_t(\gamma_t,\gamma_{t+1})} < 1$ since $d_t(\cdot,\cdot) \geq 0$.Therefore, $\log \sum_{\mathcal{G}} e^{-\beta \sum_{t=0}^{M} d_t(\gamma_t,\gamma_{t+1})} < \log|\mathcal{G}|$. The result follows since $\sum_{\gamma_0} \rho_{\gamma_0} = 1$. Part (b) of the theorem follow directly from the expression of $F$ in (12). Part (c): At the instant when $y(t) = y_c(t)$ we have that $\bar{y}(t) = 0$. Hence, the derivative of free-energy $\dot{F}(t)$ is given by $\dot{F} = x^T \hat{P}_{\gamma_0} \Phi + [z^T - y_c^T \hat{C}]\psi$, which is independent of $\bar{u}$. Hence $\frac{\partial \dot{F}}{\partial \bar{u}} = 0$.

### B. Theorem 4

Substituting $\bar{u}(t)$ (31) in $\dot{F}$ we obtain $\dot{F} = -K_0 \bar{y}^T (2\hat{A} - \hat{B})\bar{y} - (\alpha^2 + (\bar{y}(2\hat{A} - \hat{B})\bar{y})^2)^{1/2}$ where $K_0 > 0$ and $(2\hat{A} - \hat{B})$ positive definite (as shown in Appendix A). Hence $\dot{F} \leq 0$. We know from Theorem 3 that the free-energy function $F$ is lower bounded and from above we have that for the control $\bar{u}(t)$ in (31) $\dot{F} \leq 0$. We conclude from here that $F(t)$ converges (say to $F_\infty$, where $|F_\infty| < \infty$) and $|\dot{F}(t)| \to 0$ as $t \to \infty$. Now since $\dot{F} = -K_0 \bar{y}^T (2\hat{A} - \hat{B})\bar{y} - (\alpha^2 + (\bar{y}(2\hat{A} - \hat{B})\bar{y})^2)^{1/2}$, we have that $K_0 \bar{y}^T (2\hat{A} - \hat{B})\bar{y} \leq |\dot{F}|$. Thus we conclude that $\bar{y}(t) \to 0$ as $t \to \infty$.

### C. Theorem 5

Note: The proof here is similar to the proof for [35, Prop. 3.43]. Since $(2\hat{A} - \hat{B})$ and $\Phi$ are Lipschitz, it is enough to show that $\bar{u}$ is Lipschitz at $\bar{\zeta} = 0$. Since $\underline{\hat{u}} \triangleq \hat{u} - (2\hat{A} -$

$\hat{B})^{-1}(\hat{P}^0(\gamma_1,\gamma_0)^T\Phi + \hat{C}\psi)$ is Lipschitz at $\bar{\zeta}=0$, there exists a neighborhood $B_\delta \triangleq \{\bar{\zeta} : \|\bar{\zeta}\| \leq \delta\}$ and $\bar{k}>0$ such that $\|\hat{\underline{u}}(\bar{\zeta})\| \leq \bar{k}\|\bar{\zeta}\|\ \ \forall \bar{\zeta} \in B_\delta$. Also $F = \alpha + \bar{y}^T(2\hat{A}-\hat{B})\hat{\underline{u}}(t) \leq 0$ where $\alpha = [x^T\hat{P}_{\gamma_0} - y_c^T\hat{P}_0(\gamma_1|\gamma_0)^T]\Phi + [z^T - y_c^T\hat{C}]\psi$. If $\alpha>0$, then $|\alpha| \leq |\bar{y}^T(2\hat{A}-\hat{B})\hat{\underline{u}}| \leq \bar{k}_1\|\bar{y}\|\|\bar{\zeta}\|\ \forall \bar{\zeta} \in B_\delta$ where $\bar{k}_1 = k\lambda_{\max}(2\hat{A}-\hat{B})$. Thus, the control design $\bar{u}$ (31) can be bounded above as $\|\bar{u}\| \leq (2\bar{k}+K_0+1)\|\bar{\zeta}\|$. For the case when $\alpha<0$, we have that $\|\bar{u}\| \leq (1+K_0)\|\bar{y}\| \leq (1+K_0)\|\bar{\zeta}\|$.

## REFERENCES


[1] M. Barthélemy, "Spatial networks," *Phys. Rep.*, vol. 499, nos. 1–3, pp. 1–101, 2011.

[2] D. Li *et al.*, "Percolation transition in dynamical traffic network with evolving critical bottlenecks," *Proc. Nat. Acad. Sci.*, vol. 112, no. 3, pp. 669–672, 2015.

[3] D. Vaknin, M. M. Danziger, and S. Havlin, "Spreading of localized attacks in spatial multiplex networks," *New J. Phys.*, vol. 19, no. 7, 2017, Art. no. 073037.

[4] Y. Berezin, A. Bashan, M. M. Danziger, D. Li, and S. Havlin, "Localized attacks on spatially embedded networks with dependencies," *Scientific Rep.*, vol. 5, 2015, Art. no. 8934.

[5] M. Barthelemy, *Morphogenesis of Spatial Networks*. Berlin, Germany: Springer, 2018.

[6] M. Watson, *Supply Chain Network Design: Applying Optimization and Analytics to the Global Supply Chain*. London, U.K.: Pearson Education, 2013.

[7] D. Hwang, P. Jaillet, and Z. Zhou, "Distributed multi-depot routing without communications," 2014, *arXiv:1412.2123*.

[8] I. Bistritz, A. Ward, Z. Zhou, and N. Bambos, "Smart greedy distributed allocation in microgrids," in *Proc. IEEE Int. Conf. Commun.*, 2019, pp. 1–6.

[9] R. Takei, R. Tsai, Z. Zhou, and Y. Landa, "An efficient algorithm for a visibility-based surveillance-evasion game," Inst. Comput. Eng. Sci., Texas Univ. Austin, Austin, TX, USA, Tech. Rep. UTA-ICES-TR-12-06, 2012.

[10] I. F. Akyildiz, W. Su, Y. Sankarasubramaniam, and E. Cayirci, "A survey on sensor networks," *IEEE Commun. Mag.*, vol. 40, no. 8, pp. 102–114, Aug. 2002.

[11] J. Cortes, S. Martinez, T. Karatas, and F. Bullo, "Coverage control for mobile sensing networks," *IEEE Trans. Robot. Autom.*, vol. 20, no. 2, pp. 243–255, Apr. 2004.

[12] D. R. d. M. Faria, R. A. d. Santos, K. M. G. Santos, and D. H. Spadoti, "A system to improve the management of 5G and IOT networks by determining the mobile position," *J. Microw., Optoelectron. Electromagn. Appl.*, vol. 18, no. 2, pp. 293–305, 2019.

[13] A. Moustakas, P. Mertikopoulos, Z. Zhou, and N. Bambos, "Least action routing: Identifying the optimal path in a wireless relay network," in *Proc. IEEE 28th Annu. Int. Symp. Pers., Indoor, Mobile Radio Commun.*, 2017, pp. 1–5.

[14] F. Kuhn, R. Wattenhofer, and A. Zollinger, "An algorithmic approach to geographic routing in ad hoc and sensor networks," *IEEE/ACM Trans. Netw.*, vol. 16, no. 1, pp. 51–62, Feb. 2008.

[15] L. Zhou, X. Wang, L. Ni, and Y. Lin, "Location-routing problem with simultaneous home delivery and customer's pickup for city distribution of online shopping purchases," *Sustainability*, vol. 8, no. 8, 2016, Art. no. 828.

[16] M. Mahajan, P. Nimbhorkar, and K. Varadarajan, "The planar k-means problem is NP-hard," in *Proc. Int. Workshop Algorithms Comput.*, 2009, pp. 274–285.

[17] A. V. Goldberg and C. Harrelson, "Computing the shortest path: A search meets graph theory," in *Proc. 16th Annu. ACM-SIAM Symp. Discrete Algorithms*, 2005, pp. 156–165.

[18] Z. Drezner and H. W. Hamacher, *Facility Location: Applications and Theory*. Berlin, Germany: Springer, 2001.

[19] P. Sharma, S. Salapaka, and C. Beck, "A scalable approach to combinatorial library design for drug discovery," *J. Chem. Inf. Model.*, vol. 48, no. 1, pp. 27–41, 2008.

[20] Y. Xu, S. M. Salapaka, and C. L. Beck, "Aggregation of graph models and Markov chains by deterministic annealing," *IEEE Trans. Autom. Control*, vol. 59, no. 10, pp. 2807–2812, Oct. 2014.

[21] M. Baranwal, "Entropy-based framework for combinatorial optimization problems and enabling the grid of the future," Ph.D. Dissertation, Mech. Sci. Eng., Univ. Illinois Urbana-Champaign, Champaign, IL, USA, 2018.

[22] K. Rose, "Deterministic annealing for clustering, compression, classification, regression, and related optimization problems," *Proc. IEEE*, vol. 86, no. 11, pp. 2210–2239, Nov. 1998.

[23] S. Lloyd, "Least squares quantization in PCM," *IEEE Trans. Inf. Theory*, vol. IT-28, no. 2, pp. 129–137, Mar. 1982.

[24] P. Sharma, S. M. Salapaka, and C. L. Beck, "Entropy-based framework for dynamic coverage and clustering problems," *IEEE Trans. Autom. Control*, vol. 57, no. 1, pp. 135–150, Jan. 2012.

[25] Y. Wang, X. Li, and R. Ruiz, "A fast algorithm for finding the bi-objective shortest path in complicated networks," in *Proc. IEEE 22nd Int. Conf. Comput. Supported Cooperative Work Des.*, 2018, pp. 104–109.

[26] S. Okada and T. Soper, "A shortest path problem on a network with fuzzy arc lengths," *Fuzzy Sets Syst.*, vol. 109, no. 1, pp. 129–140, 2000.

[27] L. Guo, Y. Deng, K. Liao, Q. He, T. Sellis, and Z. Hu, "A fast algorithm for optimally finding partially disjoint shortest paths," in *Proc. 27th Int. Joint Conf. Artif. Intell.*, 2018, pp. 1456–1462.

[28] N. V. Kale and S. M. Salapaka, "Maximum entropy principle-based algorithm for simultaneous resource location and multihop routing in multiagent networks," *IEEE Trans. Mobile Comput.*, vol. 11, no. 4, pp. 591–602, Apr. 2012.

[29] A. Srivastava and S. M. Salapaka, "Combined resource allocation and route optimization in multiagent networks: A scalable approach," in *Proc. IEEE Amer. Control Conf.*, 2017, pp. 3956–3961.

[30] R. K. Ahuja, *Network Flows: Theory, Algorithms, and Applications*. London, U.K.: Pearson Education, 2017.

[31] A. Gersho and R. M. Gray, *Vector Quantization and Signal Compression*, vol. 159. Berlin, Germany: Springer-Verlag, 2012.

[32] C. E. Shannon and W. Weaver, *The Mathematical Theory of Communication*, Urbana, IL, USA: Univ. Illinois Press, 1949.

[33] C. E. Shannon, "A mathematical theory of communication," *ACM SIGMOBILE Mobile Comput. Commun. Rev.*, vol. 5, no. 1, pp. 3–55, 2001.

[34] E. T. Jaynes, *Probability Theory: The Logic of Science*. Cambridge, U.K.: Cambridge Univ. Press, 2003.

[35] R. Sepulchre, M. Jankovic, and P. V. Kokotovic, *Constructive Nonlinear Control*. Berlin, Germany: Springer, 2012.

[36] E. D. Sontag, "A Lyapunov-like characterization of asymptotic controllability," *SIAM J. Control Optim.*, vol. 21, no. 3, pp. 462–471, 1983.

[37] E. D. Sontag, "A 'universal'construction of Artstein's theorem on nonlinear stabilization," *Syst. Control Lett.*, vol. 13, no. 2, pp. 117–123, 1989.

[38] R. S. Varga, *Geršgorin and His Circles*. Berlin, Germany: Springer-Verlag, 2010, vol. 36.


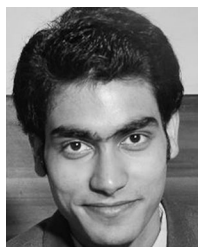

**Amber Srivastava** received the B.Tech. degree in mechanical engineering from the Indian Institute of Technology, Kanpur, India, in 2014. Currently, he is working toward the Ph.D. degree with the University of Illinois at Urbana Champaign (UIUC), Champaign, IL, USA.

He was with an FMCG in India for an year (2014–2015) as an Assistant Manager. His research interests include optimization, reinforcement learning, and controls.

**Srinivasa M. Salapaka** (Member, IEEE) received the B.Tech. degree in mechanical engineering from the Indian Institute of Technology, Chennai, India, in 1995, and the M.S. and Ph.D. degrees in mechanical engineering from the University of California, Santa Barbara, CA, USA, in 1997 and 2002, respectively.

From 2002 to 2004, he was a Postdoctoral Associate with the Laboratory for Information and Decision Systems, Massachusetts Institute of Technology, Cambridge, MA, USA. Since 2004, he has been a Faculty Member with the Mechanical Science and Engineering Department, University of Illinois, Urbana-Champaign, IL, USA. His research interests include controls for nanotechnology, combinatorial facility allocation, and power electronics.

Dr. Salapaka was the recipient of the NSF CAREER Award in 2005 and is an ASME Fellow since 2015.